Acta Crystallographica Section D
Biological Crystallography
ISSN 0907-4449

Structure of Greyhound hemoglobin: origin of high oxygen affinity

Veer S. Bhatt,[a] Sara Zaldívar-López,[b] David R. Harris,[c] C. Guillermo Couto,[b] Peng G. Wang[d]* and Andre F. Palmer[c]*

[a]Biophysics Graduate Program, The Ohio State University, Columbus, OH 43210, USA, [b]Department of Veterinary Clinical Sciences, College of Veterinary Medicine, The Ohio State University, Columbus, OH 43210, USA, [c]William G. Lowrie Department of Chemical and Biomolecular Engineering, The Ohio State University, Columbus, OH 43210, USA, and [d]Department of Biochemistry, Department of Chemistry, The Ohio State University, Columbus, OH 43210, USA

Correspondence e-mail: wang.892@osu.edu, palmer@chbmeng.ohio-state.edu

Received 2 June 2010
Accepted 17 February 2011

PDB Reference: Greyhound hemoglobin, 3pel.

This study presents the crystal structure of Greyhound hemoglobin (GrHb) determined to 1.9 Å resolution. GrHb was found to crystallize with an $\alpha_1\beta_1$ dimer in the asymmetric unit and belongs to the R2 state. Oxygen-affinity measurements combined with the fact that GrHb crystallizes in the R2 state despite the high-salt conditions used for crystallization strongly indicate that GrHb can serve as a model high-oxygen-affinity hemoglobin (Hb) for higher mammals, especially humans. Structural analysis of GrHb and its comparison with the R2-state of human Hb revealed several regions that can potentially contribute to the high oxygen affinity of GrHb and serve to rationalize the additional stability of the R2-state of GrHb. A previously well studied hydrophobic cluster of bar-headed goose Hb near α119 was also incorporated in the comparison between GrHb and human Hb. Finally, a structural comparison with generic dog Hb and maned wolf Hb was conducted, revealing that in contrast to GrHb these structures belong to the R state of Hb and raising the intriguing possibility of an additional allosteric factor co-purifying with GrHb that can modulate its quaternary structure.

1. Introduction

Hemoglobin (Hb) has been investigated for diverse applications ranging from the development of oxygen therapeutics (*i.e.* red blood cell substitutes) to serving as a model for molecular disease and allostery (Schechter, 2008; Perutz, 1979; Shaanan, 1983; Mueser *et al.*, 2000). In general, Hbs can be classified into two groups on the basis of intrinsic oxygen affinity: those with high oxygen affinity such as those from dogs, rodents, camels and most primates, and those with low oxygen affinity such as those from cows, sheep, goats and deer. In this work, we seek to relate the structure of Greyhound Hb (GrHb) to its high oxygen affinity. The polypeptide sequence of GrHb is 100% identical to that of generic dog (*Canis lupus familiaris*) Hb and hence the structure may also represent the structure of generic dog Hb, to which a similar analysis can then be extrapolated. The GrHb structure can in turn serve as a structural model of a high-oxygen-affinity Hb such as human Hb (HuHb).

Hb is a tetrameric protein ($\alpha_2\beta_2$) with a dyad axis. It is known to exist in several quaternary states depending on whether it is unliganded or liganded. The quaternary state of unliganded Hb is characterized by its low oxygen affinity and is referred to as the tense (T) state. Recent findings suggest that Hb can access an ensemble of T states (Biswal & Vijayan, 2002). Several quaternary states of liganded Hb such as relaxed (R), R2, B and Y have also been reported in the literature (Silva *et al.*, 1992; Smith & Simmons, 1994; Kroeger

& Kundrot, 1997; Schumacher *et al.*, 1997; Pairet & Jaenicke, 2010). In this work, we will restrict our discussion to the R and R2 states of Hb. The R2 state was initially proposed to serve as an intermediate between the T and R states (Silva *et al.*, 1992). Later, it was shown to be more likely to represent the end state of the liganded Hb (Schumacher *et al.*, 1997). These quaternary states are defined by the relative orientation of the $\alpha_1\beta_1$ subunit to the $\alpha_2\beta_2$ subunit and thus also by the $\alpha_1\beta_2$ interface. The $\alpha_1\beta_2$ (and corresponding $\alpha_2\beta_1$) interface acts as a molecular slide bearing from which Hb can adopt conformations with high or low oxygen affinity (Perutz, 1979; Shaanan, 1983). More recent work illustrated that the $\alpha_1\beta_1$ (and corresponding $\alpha_2\beta_2$) interface is also important in modulating oxygen affinity (Zhang *et al.*, 1996; Liang *et al.*, 2001; Tsai & Ho, 2002). Additionally, it was shown that interactions at the C-termini in the central cavity of Hb are also critical in regulating oxygen affinity. Thus, in HuHb it was found that these termini have a greater degree of freedom in the R state relative to the T state (Shaanan, 1983). In bovine Hb (BvHb) it was found that halide ions can diffuse into the central cavity to reduce charge repulsions arising from positively charged residues and hence preferentially stabilize the T state (Perutz *et al.*, 1993). Allosteric effectors were also found to play an important role in regulating the oxygen affinity of Hb. These effectors may be universal, for example H^+ ions (Bonaventura *et al.*, 1974), or may vary across species; for example, 2,3-diphosphoglycerate (2,3-DPG) regulates oxygen affinity in dogs, rodents and most primates (Bunn, 1971), while halide ions regulate oxygen affinity in ruminants (Bonaventura *et al.*, 1974) and inositol pentaphosphate (IPP) regulates oxygen affinity in birds (Taketa, 1974; Zhang *et al.*, 1996). In light of this, several questions arose. Can the high oxygen affinity of GrHb be rationalized on the above-mentioned grounds (*i.e.* $\alpha_n\beta_n$-type intersubunit interactions, interactions in the central cavity and interactions induced by secondary effectors)? How does the intrinsic oxygen affinity of GrHb compare with that of HuHb, both of which are high-oxygen-affinity Hbs? What specific liganded state does GrHb correspond to? Could this have a bearing on its oxygen affinity? What regions of the GrHb structure could be most critical in defining the observed high oxygen affinity? How do these regions compare with other Hbs with high oxygen affinity, especially HuHb?

In this work, we will compare the intrinsic oxygen affinity of GrHb with that of HuHb. We then present the crystal structure of GrHb at a resolution of 1.9 Å and attempt to investigate these questions by incorporating details from previously reported Hb structures, namely the R2 state of HuHb (HuHb; Silva *et al.*, 1992; PDB entry 1bbb), the R state of HuHb (RHuHb; Shaanan, 1983; PDB entry 1hho), the R2 state of guinea pig Hb (PiHb; Pairet & Jaenicke, 2010; PDB entry 3hyu), bar-headed goose Hb (BaHb; Zhang *et al.*, 1996; PDB entry 1a4f), maned wolf Hb (MwHb; Fadel *et al.*, 2003; PDB entry 1fhj) and generic dog Hb (S. S. Sundaresan, P. Ramesh, M. Thenmozhi & M. N. Ponnuswamy, unpublished work; PDB entry 3gou).

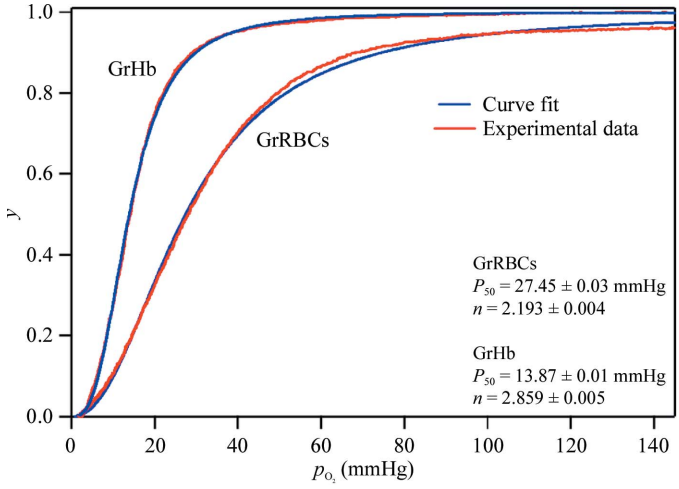

Figure 1
O_2–GrRBC/GrHb equilibrium curves measured at 310 K.

2. Materials and methods

2.1. Purification of GrHb and measurement of oxygen affinity

GrHb was purified from Greyhound red blood cells (GrRBCs) *via* tangential flow filtration according to the literature (Palmer *et al.*, 2009; Elmer *et al.*, 2009). The O_2–GrRBC/GrHb equilibrium curve was measured at 310 K using a Hemox Analyzer as previously described in the literature (Palmer *et al.*, 2009). The O_2–GrRBC/GrHb equilibrium curve was then fitted to the Hill equation to regress the P_{50} [*i.e.* the partial pressure of oxygen (p_{O_2}) at which the Hb is half-saturated with oxygen] and cooperativity coefficient (n; Palmer *et al.*, 2009) and is shown in Fig. 1.

2.2. Crystallization of GrHb, data collection and processing

GrHb was concentrated to 100 mg ml^{-1}, centrifuged to remove any precipitate and then used to search for conditions that could lead to crystallization using commercial screens (Hampton Research, California, USA). The first crystals were obtained in 1.6–2.4 *M* ammonium sulfate, 100 m*M* Tris pH 8.5. The best diffracting crystals were obtained after optimization using additive screens (Hampton Research, California, USA) in a sitting-drop vapor-diffusion setup, in which 5 µl GrHb was mixed with 5 µl crystallization reagent [1.7 *M* ammonium sulfate, 100 m*M* glycine pH 9.0, 0.6 *M* 3-(1-pyridino)-1-propane sulfonate (NDSB-201) and 21% glycerol] and allowed to equilibrate against well solution (500 µl 1.7 *M* ammonium sulfate, 100 m*M* glycine pH 9.0, 21% glycerol). The crystals grew to full size in less than two weeks and were then transferred to cryoprotection buffer (1.7 *M* ammonium sulfate, 100 m*M* glycine pH 9.0, 0.6 *M* NDSB-201, 30% glycerol), flash-frozen in nylon cryoloops (Hampton Research, California, USA) and stored in liquid nitrogen. A 1.9 Å resolution data set was collected at 113 K using an R-AXIS IV^{++} imaging-plate detector and Cu $K\alpha$ radiation generated by a rotating-anode X-ray generator (Rigaku–MSC, Texas,

Table 1
Data-collection and refinement statistics.

Values in parentheses are for the highest resolution shell.

Data-collection statistics	
Source	Cu $K\alpha$
Space group	$C2$
Unit-cell parameters (Å, °)	$a = b = 88.0$, $c = 53.1$, $\alpha = \gamma = 90.0$, $\beta = 103.4$
Temperature (K)	113.15
Wavelength (Å)	1.5
Resolution (Å)	33.50–1.90 (1.97–1.90)
$R_{\rm merge}$†	0.037 (0.100)
Completeness (%)	99.6 (96.4)
$\langle I/\sigma(I)\rangle$	23.7 (9.4)
Total No. of reflections	115162
No. of unique reflections	31041
Average multiplicity	3.71 (3.22)
Mosaicity (°)	0.63
B factor from Wilson plot (Å^2)	18.5
PDB entry	3pel
Refinement statistics	
Resolution (Å)	33.50–1.90
No. of reflections	29475
R factor‡	0.19
$R_{\rm free}$‡	0.23
No. of protein atoms	
α-Subunit	1076
β-Subunit	1150
No. of water atoms	452
No. of ligand atoms (heme, Fe^{2+}, water)	86
R.m.s. deviation from ideal values§	
Bond distances (Å)	0.006
Bond angles (°)	0.873
Average B factors (Å^2)	
Main chain	15.5
Side chain and waters	21.0
All atoms	18.6
Ramachandran plot¶	
Favored (%)	98.9
Disallowed (%)	0

† $R_{\rm merge} = \sum_{hkl}\sum_i |I_i(hkl) - \langle I(hkl)\rangle| / \sum_{hkl}\sum_i I_i(hkl)$. ‡ R factor $= \sum_{hkl} ||F_{\rm obs}| - |F_{\rm calc}|| / \sum_{hkl} |F_{\rm obs}|$; $R_{\rm free}$ is the R factor for 5% of the data that were excluded from refinement. § Ideal values from Engh & Huber (1991) were used. ¶ Validation by *MolProbity* (Chen *et al.*, 2010).

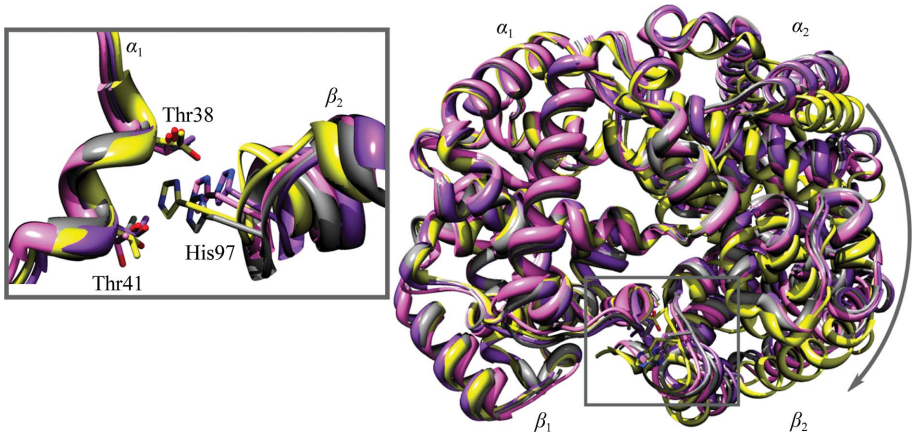

Figure 2
GrHb is in the R2 state. Structural alignment of $\alpha_1\beta_1$ subunits of the tetramer of GrHb (gray) with the R2 state of HuHb (purple), the R state of HuHb (yellow) and the R2 state of PiHb (pink) shows that GrHb belongs to the R2 state. The relative rotation of the $\alpha_2\beta_2$ subunits is highlighted by the curved arrow and the relative orientation of the residues α_1Thr38, α_1Thr41 and β_2His97 in the structural alignment is highlighted in the inset.

USA) operating at 46 kV and 90 mA. The temperature was maintained during data collection using an X-STREAM cryogenic device (Rigaku-MSC, Texas, USA). The data were processed, integrated and scaled with *CrystalClear* software (Rigaku–MSC, Texas, USA). The data-processing statistics are listed in Table 1.

2.3. Structure determination of GrHb

A sequence alignment was generated between GrHb and equine Hb (EqHb; Mueser *et al.*, 2000; PDB entry 1g0b) using *ClustalW* (Thompson *et al.*, 2002). A search model was prepared from the crystal structure of EqHb by mutating the mismatched residues to alanines. Molecular replacement using *AMoRe* (Navaza, 2001) was then used to find a solution to the phase problem using this search model. A unique solution could be obtained in the same space group with a dimer in the asymmetric unit. This solution had a Matthews coefficient ($V_{\rm M}$) of 3.12 Å^3 Da^{-1}, corresponding to a solvent content of 61%. It had an R factor of 0.40 and a correlation coefficient of 0.64, which were clearly distinct from the next best solution (R factor of 0.53 and correlation coefficient of 0.43). Several cycles of maximum-likelihood-based refinement reduced the R factor and $R_{\rm free}$ to 0.29 and 0.31, respectively. The $R_{\rm free}$ was calculated from a set comprised of 5% of all reflections. All refinement was conducted using *REFMAC* (Murshudov *et al.*, 1997) with a diagonal weighting of 0.03. In the first round of model building using *Coot* (Emsley & Cowtan, 2004), variations were made in this refined model according to the amino-acid sequence of generic dog Hb. At the same time, modifications in the main-chain and side-chain positions were made according to the $2F_{\rm o} - F_{\rm c}$ electron-density map. The model was then subjected to five further cycles of refinement, which reduced the R factor and $R_{\rm free}$ to 0.23 and 0.27, respectively. Next, solvent molecules (H_2O) were added followed by a round of refinement performed in a similar fashion as described above. A final round of manual model building was carried out according to newly revealed details in the $2F_{\rm o} - F_{\rm c}$ electron-density map followed by a last round of *REFMAC* refinement. *MolProbity* (Chen *et al.*, 2010) was used to validate the quality of the final model. Details of the data processing, final refinement and validation statistics are listed in Table 1.

2.4. LC-MS/MS analysis of GrHb

Capillary–liquid chromatography–nanospray tandem mass spectrometry (Nano-LC/MS/MS) was performed on trypsin-digested GrHb samples at the Mass Spectrometry and Proteomics Facility of the Campus Chemical Instrument Center (The Ohio State University, Columbus, Ohio, USA)

using a Thermo Finnigan LTQ mass spectrometer equipped with a nanospray source. Sequence information from the MS/MS data was searched using *Mascot Daemon* software (Boston, Massachusetts, USA) using the full Swiss-Prot database v.57.5 or NCBI database v.20091013. The fragments giving a 'score' of 50 or more were considered to be positive matches towards the corresponding proteins. The polypeptide sequence thus obtained was further validated in the $2F_o - F_c$ electron-density map.

2.5. Structure comparison

In order to deduce the quaternary state to which the GrHb crystal structure corresponds, structural alignments were carried out with several available R-state and R2-state structures. The R state of HuHb was used as the structure representing the R state of Hb. The structures of the R2 state of HuHb and PiHb were used as structures representing the R2 state of Hb. The alignments were carried out by superimposing the corresponding C^{α} atoms of the $\alpha_1\beta_1$ subunits of the structures being compared and then observing the overall displacement in the corresponding $\alpha_2\beta_2$ subunits, especially in the region where α_1Thr38, α_1Thr41 and β_2His97 interact (Fig. 2). Structural alignments were carried out using *UCSF Chimera* (Pettersen *et al.*, 2004), with the tetrameric forms obtained using *Swiss-PdbViewer* (Guex & Peitsch, 1997) when required. The residues/regions deemed to be most important and discussed in this work are highlighted in a structure-based sequence alignment produced by *UCSF Chimera* (Pettersen *et al.*, 2004; Fig. 3). Following this, a structural analysis was carried out between GrHb and HuHb (R2 state). Interactions at a hydrophobic region near residue α119 were then analyzed between GrHb, HuHb and BaHb. This region has previously been reported to be important in modulating oxygen affinity. The reported structures of MwHb and generic dog Hb were finally incorporated into these analyses to compare the corresponding quaternary states. All molecular graphics and the structure-based sequence alignment were prepared using *UCSF Chimera* (Pettersen *et al.*, 2004).

3. Results

3.1. Oxygen affinity of GrHb

Measurement of the intrinsic oxygen affinity of GrHb revealed that its P_{50} is $\sim$13.87 $\pm$ 0.01 mmHg (1 mmHg = 133.3 Pa) and its cooperativity coefficient (n) is 2.859 $\pm$ 0.005 (Fig. 1). This value is very similar to the value of 13.57 mmHg reported for HuHb purified using the same methodology (tangential flow filtration; Palmer *et al.*, 2009).

3.2. Overall structure

The final model of GrHb consists of one $\alpha_1\beta_1$ dimer of the R2 state of GrHb in the methemoglobin (metHb) form with a total of 452 water molecules. The α_1 subunit is comprised of 141 residues and the β_1 subunit is comprised of 146 residues. The electron density is very well defined (Fig. 4) for all residues other than αVal1, αLys16, αLys86, αAla130, βAsp43 and βAla87. The polypeptide sequence of GrHb obtained by Nano-LC/MS/MS as described in §2 was validated using the $2F_o - F_c$ electron-density map. The sequence is identical to that of generic dog (*i.e. C. lupus familiaris*) Hb (PDB entry

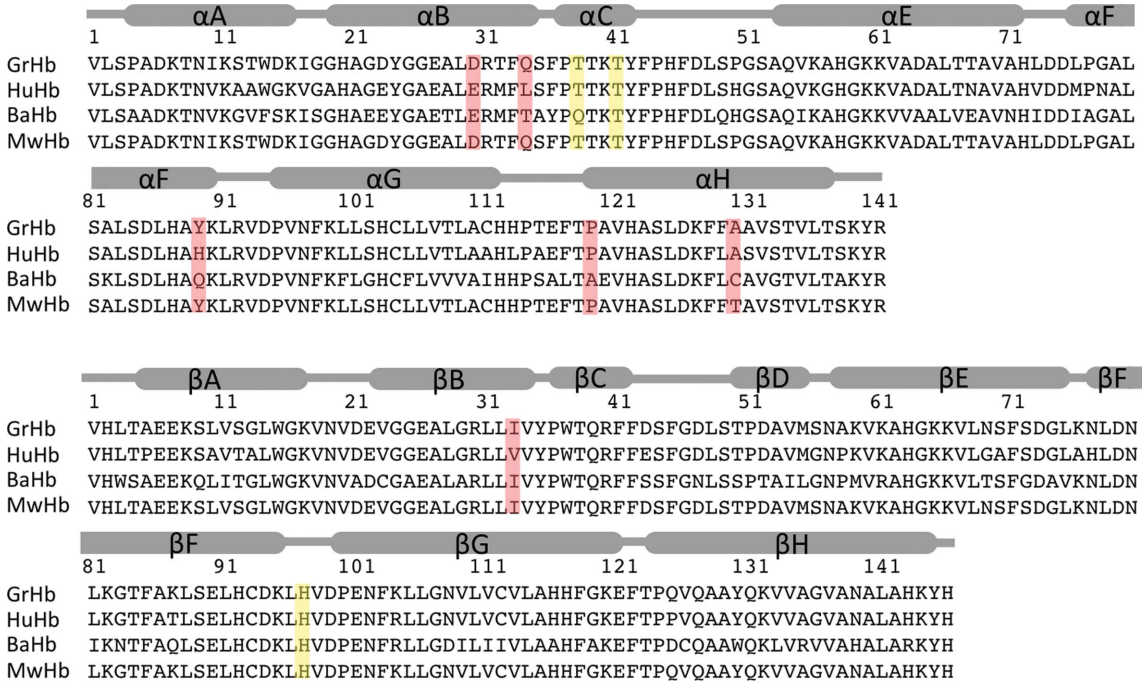

Figure 3
Structure-based multiple sequence alignment. α-Subunits (top) and β-subunits (bottom) from GrHb, HuHb, BaHb and MwHb are aligned. The variations proposed to be important in this work are highlighted in salmon. The residues that are important in assignment of the specific quaternary state are highlighted in yellow.

3gou; Sundaresan *et al.*, unpublished work). However, we still distinguish it as GrHb since GrHb exhibits a distinctly higher oxygen affinity than generic dog Hb (Sullivan *et al.*, 1994). MwHb is also a very close relative of GrHb. The sequence identity between GrHb and MwHb is close to 100%, with the only variation being that αAla130 in GrHb is replaced by Thr in MwHb. Sequence comparisons of GrHb with HuHb and BaHb revealed overall sequence identities of ∼86% and ∼69%, respectively.

3.3. GrHb represents the R2 state of Hb

Comparison of the structure of GrHb with Hbs in different quaternary states revealed that the GrHb crystal structure is that of the R2 state. This is clear from a superposition of the $\alpha_1\beta_1$ subunits of the structures of the R2 states of HuHb and PiHb and the R state of HuHb with the $\alpha_1\beta_1$ subunit of GrHb and the corresponding positions of the interface between α_1Thr38, α_1Thr41 and β_2His97 (Fig. 2). The electron density and the geometry of the ligand-binding pocket is suggestive of a water molecule instead of an oxygen ligand and hence the structure of GrHb is that of the R2 state in the met form (Fig. 4). The R2 state is typically observed under crystallization conditions characterized by low salt concentrations, with the only exception reported to our knowledge being that of PiHb (Pairet & Jaenicke, 2010). In this regard, GrHb may also be considered exceptional since it crystallizes in the R2 state despite the high salt conditions used for crystallization. This fact may have important implications as discussed below.

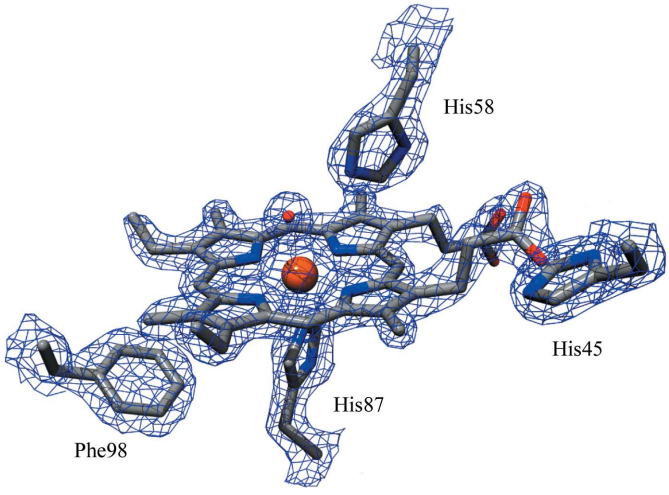

Figure 4
Representative electron density of GrHb. $2mF_o - DF_c$ electron-density map contoured at an absolute electron density of 1.07 e Å^{-3} (1.5σ cutoff) showing the α-subunit heme and a water molecule bound to Fe^{3+}.

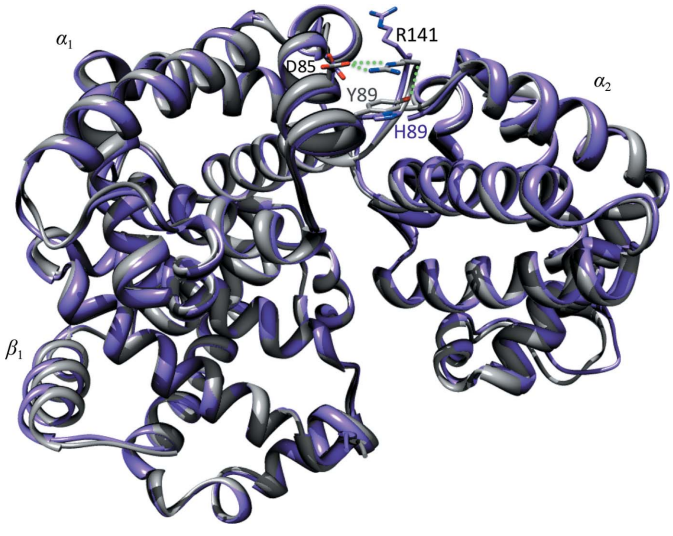

Figure 5
Restricted conformation of the α C-termini of GrHb relative to HuHb. A variation from αHis89 in HuHb (purple) to Tyr in GrHb results in the formation of van der Waals stacking interactions as well as a hydrogen-bond network at the α C-termini of GrHb. This in turn could possibly restrict the transition from the liganded (R or R2) to the unliganded (T) states. Dotted green lines represent hydrogen bonds.

4. Discussion

Hb has been a protein of interest for several decades not only because of its ability to serve as a precursor for oxygen therapeutic synthesis/formulation but also because of its intriguing properties at the molecular level such as its multiple quaternary states and its structural modulation by H^+ ions and other allosteric effectors. The oxygen affinity of Hb is modulated by $\alpha_n\beta_n$-type interactions, salt bridges formed between the C-termini of the α and β subunits and by several allosteric effectors as discussed in detail in §1 above. In this study, GrHb was found to crystallize in the R2 state. The R2 state of Hb was initially thought to be an intermediate between the T and R states (Silva *et al.*, 1992), but was finally reported to represent the 'end state' of the liganded Hb (Schumacher *et al.*, 1997), hence making it physiologically more relevant. Typically, the R2 state has only been obtained only under low-salt conditions, thereby reinforcing its physiological importance. The only exception reported to date in this regard is that of altitude-adapted Hb derived from guinea pigs (Pairet & Jaenicke, 2010). Thus, the fact that GrHb crystallizes in the R2 state despite the high salt concentration used for crystallization reflects the relatively high stability of the R2 state of GrHb when compared with the R2 state of other Hbs, especially the R2 state of HuHb. Drawing upon all these ideas, we investigated the 1.9 Å resolution structure of the R2 state of GrHb to infer structural features that could lead to its high oxygen affinity.

While comparing the structures of the R2 state of GrHb and the R2 state of HuHb we found several sets of interactions that can rationalize the additional stability of the R2 state of GrHb over the R2 state of HuHb. These interactions could also be important in enabling GrHb to crystallize in the R2 state despite the high salt concentration. The first set of interactions is present between α_1Tyr89, α_1Arg141 and α_1Asp85. It originates out of a variation from α_1His89[1] in HuHb to Tyr in GrHb. α_1Tyr89 in turn forms van der Waals stacking interactions with the C-terminal α_1Arg141 (Fig. 5). A weak hydrogen bond (3.4 Å) is also present between the side-

[1] All residue numbering corresponds to GrHb, unless stated otherwise.

chain OH of α_1Tyr89 and the main-chain NH group of the C-terminal α_1Arg141. As a consequence of these interactions, the side chain of α_1Arg141 is in a position to make two hydrogen bonds to α_1Asp85 $O^{\delta1}$ (~2.7 and ~3.4 Å; Fig. 5), thereby restricting the α C-termini from participating in the intersubunit salt bridges that are required for transition to the T state. Although the α C-terminus of the R2 state of HuHb has a similar conformation, these additional interactions at the α C-terminus of GrHb clearly provide additional stability to the R2 state of GrHb and are very likely to make an important contribution to the crystallization of GrHb in the R2 state despite the high-salt conditions. In general, electrostatic interactions mediated by C-termini were first proposed (Perutz & Greer, 1970; Shaanan, 1983) and eventually proved (Bettati *et al.*, 1998) to be critical in stabilizing the T state of HuHb. In these investigations, the C-termini of the R state of HuHb were observed to have a greater degree of freedom than that of T-state Hb. Specifically, α C-termini arginines and β C-termini histidines were found to be involved in intersubunit salt bridges. Hence, the decreased availability of these C-terminal carboxyl groups can immediately lead to additional stability of the R2 state of GrHb relative to the R2 state of HuHb. It is to be noted that the electron density at the Asp85 side chain is not very well defined in the OMIT map (Fig. 6). Hence, the length of the hydrogen bonds is only approximate. The next set of interactions unique to GrHb is a consequence of three variations that lead to the formation of a water-mediated hydrogen-bond network at the $\alpha_1\beta_1$ interface in GrHb which is absent in HuHb. The water-mediated hydrogen-bond network forms between α_1Asp30 (Glu in HuHb), α_1Gln34 (Leu in HuHb) and β_1Gln125 (Pro in HuHb) (Fig. 7) and in addition a weak hydrogen bond (3.5 Å) also forms between the side chain of α_1Gln34 and the main-chain NH group of β_1Gln125. The presence of this hydrogen-bond network thus further reduces the free energy of the R2 state of GrHb relative to the R2 state of HuHb. Although we could not find any literature specifically regarding the investigation of this region, the $\alpha_1\beta_1$ interface itself has been often implicated as being critical in modulating oxygen affinity (Zhang *et al.*, 1996; Liang *et al.*, 2001; Tsai & Ho, 2002; Jessen *et al.*, 1991) and water-mediated hydrogen bonds at subunit interfaces have generally been reported to play a key role in oligomeric stability (Schreiber & Fersht, 1995; Puius *et al.*, 1998). Finally, a variation from βVal33 in HuHb to Ile in GrHb could also play an important role in imparting high oxygen affinity to GrHb. This region is discussed below in relevance to BaHb.

BaHb was incorporated in the abovementioned comparison between GrHb and HuHb because of a previously reported intriguing set of investigations. α119, which is a Pro in HuHb and an Ala in goose Hb, was first proposed by Perutz (1983) and then shown by Jessen *et al.* (1991) and Weber *et al.* (1993) to be critical in modulating oxygen affinity, citing evidence from their site-directed mutagenesis experiments. These findings were further reinforced by Zhang *et al.* (1996) and Liang *et al.* (2001) using the crystal structures of the oxy and deoxy forms of BaHb. Briefly, these experiments indicated that αPro119 is involved in the formation of critical hydrophobic interactions at the $\alpha_1\beta_1$ interface in the deoxy form of HuHb (T state), thereby stabilizing it. When this residue is mutated to Ala in HuHb (Ala being present at this position in BaHb) the corresponding deoxy form becomes relatively less stable, thereby increasing the oxygen affinity. In our comparison of GrHb with BaHb and HuHb we found that Pro is retained at the α119 position in GrHb and it participates in a hydrophobic cluster formed at the $\alpha_1\beta_1$ interface between αPro119, α123Ala, βMet55 and βIle33 (Fig. 8). However, βIle33 in GrHb is replaced by Val in HuHb, while being conserved in BaHb. The variation from βVal33 in HuHb to Ile in GrHb makes the corresponding hydrophobic interactions slightly stronger in GrHb. Given the facts that this hydrophobic cluster is at an intersubunit interface and that it is close

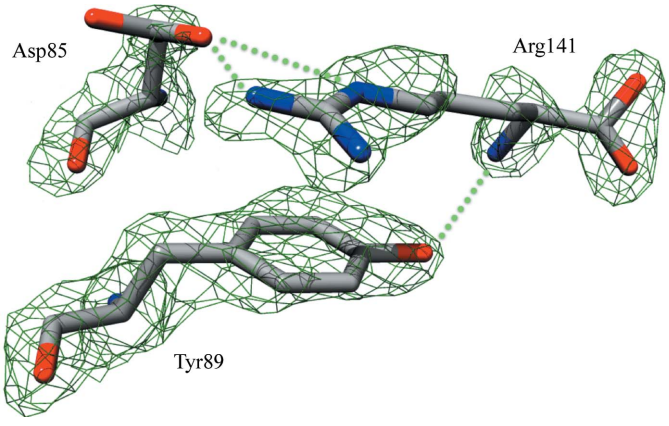

Figure 6
Composite $2mF_o - DF_c$ OMIT map at the α C-terminus of GrHb contoured at an absolute electron density of 0.22 e Å^{-3} (0.9σ cutoff). The map was produced using *PHENIX* (Terwilliger *et al.*, 2008).

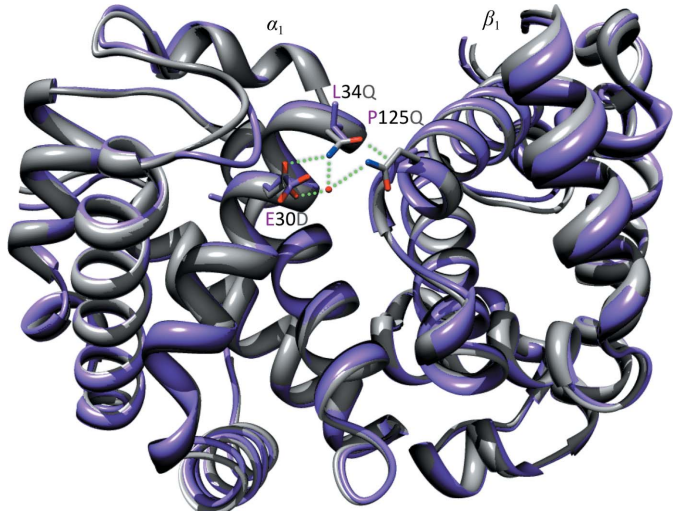

Figure 7
A water-mediated hydrogen-bond network is uniquely present in GrHb. A group of three variations, αAsp30 in GrHb replacing Glu in HuHb, αGln34 in GrHb replacing Leu in HuHb and βGln125 in GrHb replacing Pro in HuHb, creates a water-mediated hydrogen-bond network at the $\alpha_1\beta_1$ interface of GrHb (gray), hence lowering its free energy relative to the R2 state of HuHb (purple).

to the solvent-exposed surface, it is not surprising that the abovementioned investigations have validated its importance. Hence, the slightly stronger hydrophobic interactions in this region in the R2 state of GrHb relative to the R2 state of HuHb could make an important contribution to the relatively higher stability of the R2 state of GrHb.

Structural comparison of GrHb with MwHb revealed that despite the absence of salt in the crystallization mixture (Smarra *et al.*, 1999) and despite the variation of only one residue per $\alpha_1\beta_1$ dimer (α130Ala in GrHb to Thr in MwHb) the crystal structure of MwHb belongs to the R state. The one and only variation of αThr130 in MwHb to Ala in GrHb could be responsible for this, since the variation from Ala to Thr places the αArg141 side chain with several van der Waals contacts to αThr130 (data not shown). However, given the absence of a distinct hydrogen bond originating from this variation there is considerable uncertainty to this possibility. Nevertheless, this finding does reinforce the importance of the C-termini in the modulation of oxygen affinity. Our comparison with the unpublished crystal structure of generic dog Hb revealed that it also belongs to the R state, although the structure is at a much lower resolution (3.0 Å) than that of GrHb (1.9 Å). Given the 100% sequence identity between GrHb and generic dog Hb and the fact that GrHb can crystallize in the R2 state even under high-salt conditions, it is surprising that the generic dog Hb structure belongs to the R state. However, it is not possible to rationalize this in the absence of substantial details of the underlying experimental methodology.

In summary, our investigation reveals that GrHb crystallizes in the R2 state despite the high-salt conditions used for crystallization. The structural analysis of GrHb and its comparison with HuHb and BaHb reveal specific interactions that could potentially contribute to the high oxygen affinity of GrHb and also rationalize the crystallization of GrHb in the R2 state under high-salt conditions. Comparisons of GrHb with the generic dog Hb structure and MwHb reveal that despite the sequence identity (100% to generic dog Hb and ∼100% to MwHb) both of these structures belong to the R state, unlike GrHb which belongs to the R2 state. This raises the intriguing possibility of an additional factor copurifying with GrHb that can modulate its quaternary structure, which would require further experimental investigations. Overall, these analyses strongly indicate that GrHb can serve as a model system for the further investigation and design of high-oxygen-affinity Hbs.

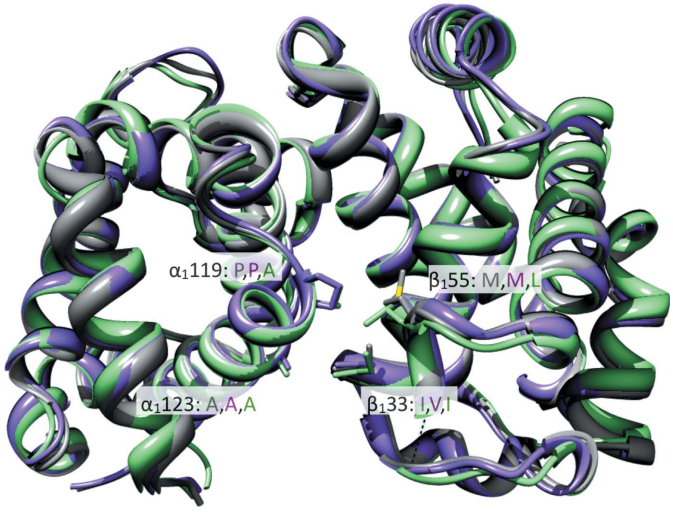

Figure 8
Hydrophobic cluster at the $\alpha_1\beta_1$ interface. A variation from αVal33 in HuHb (purple) to Ile in GrHb (gray) and BaHb (green) leads to a stronger hydrophobic interaction at the $\alpha_1\beta_1$ interface of GrHb compared with HuHb.

References

Bettati, S., Mozzarelli, A. & Perutz, M. F. (1998). *J. Mol. Biol.* **281**, 581–585.
Biswal, B. K. & Vijayan, M. (2002). *Acta Cryst.* D**58**, 1155–1161.
Bonaventura, C., Sullivan, B. & Bonaventura, J. (1974). *J. Biol. Chem.* **249**, 3768–3775.
Bunn, H. F. (1971). *Science*, **172**, 1049–1050.
Chen, V. B., Arendall, W. B., Headd, J. J., Keedy, D. A., Immormino, R. M., Kapral, G. J., Murray, L. W., Richardson, J. S. & Richardson, D. C. (2010). *Acta Cryst.* D**66**, 12–21.
Elmer, J., Harris, D. R., Sun, G. & Palmer, A. F. (2009). *Biotechnol. Prog.* **25**, 1402–1410.
Emsley, P. & Cowtan, K. (2004). *Acta Cryst.* D**60**, 2126–2132.
Engh, R. A. & Huber, R. (1991). *Acta Cryst.* A**47**, 392–400.
Fadel, V., Canduri, F., Olivieri, J. R., Smarra, A. L., Colombo, M. F., Bonilla-Rodriguez, G. O. & de Azevedo, W. F. (2003). *Protein Pept. Lett.* **10**, 551–559.
Guex, N. & Peitsch, M. C. (1997). *Electrophoresis*, **18**, 2714–2723.
Jessen, T. H., Weber, R. E., Fermi, G., Tame, J. & Braunitzer, G. (1991). *Proc. Natl Acad. Sci. USA*, **88**, 6519–6522.
Kroeger, K. S. & Kundrot, C. E. (1997). *Structure*, **5**, 227–237.
Liang, Y., Hua, Z., Liang, X., Xu, Q. & Lu, G. (2001). *J. Mol. Biol.* **313**, 123–137.
Mueser, T. C., Rogers, P. H. & Arnone, A. (2000). *Biochemistry*, **39**, 15353–15364.
Murshudov, G. N., Vagin, A. A. & Dodson, E. J. (1997). *Acta Cryst.* D**53**, 240–255.
Navaza, J. (2001). *Acta Cryst.* D**57**, 1367–1372.
Pairet, B. & Jaenicke, E. (2010). *PLoS One*, **5**, e12389.
Palmer, A. F., Sun, G. & Harris, D. R. (2009). *Biotechnol. Prog.* **25**, 189–199.
Perutz, M. F. (1979). *Annu. Rev. Biochem.* **48**, 327–386.
Perutz, M. F. (1983). *Mol. Biol. Evol.* **1**, 1–28.
Perutz, M. F., Fermi, G., Poyart, C., Pagnier, J. & Kister, J. (1993). *J. Mol. Biol.* **233**, 536–545.
Perutz, M. F. & Greer, J. (1970). *Biochem. J.* **119**, 31P.
Pettersen, E. F., Goddard, T. D., Huang, C. C., Couch, G. S., Greenblatt, D. M., Meng, E. C. & Ferrin, T. E. (2004). *J. Comput. Chem.* **25**, 1605–1612.
Puius, Y. A., Zou, M., Ho, N. T., Ho, C. & Almo, S. C. (1998). *Biochemistry*, **37**, 9258–9265.
Schechter, A. N. (2008). *Blood*, **112**, 3927–3938.
Schreiber, G. & Fersht, A. R. (1995). *J. Mol. Biol.* **248**, 478–486.
Schumacher, M. A., Zheleznova, E. E., Poundstone, K. S., Kluger, R., Jones, R. T. & Brennan, R. G. (1997). *Proc. Natl Acad. Sci. USA*, **94**, 7841–7844.
Shaanan, B. (1983). *J. Mol. Biol.* **171**, 31–59.
Silva, M. M., Rogers, P. H. & Arnone, A. (1992). *J. Biol. Chem.* **267**, 17248–17256.
Smarra, A. L. S., Fadel, V., Dellamano, M., Olivieri, J. R., de Azevedo, W. F. & Bonilla-Rodriguez, G. O. (1999). *Acta Cryst.* D**55**, 1618–1619.

Smith, F. R. & Simmons, K. C. (1994). *Proteins*, **18**, 295–300.
Sullivan, P. S., Evans, H. L. & McDonald, T. P. (1994). *J. Am. Vet. Med. Assoc.* **205**, 838–841.
Taketa, F. (1974). *Ann. N. Y. Acad. Sci.* **241**, 524–537.
Terwilliger, T. C., Grosse-Kunstleve, R. W., Afonine, P. V., Moriarty, N. W., Adams, P. D., Read, R. J., Zwart, P. H. & Hung, L.-W. (2008). *Acta Cryst.* D**64**, 515–524.
Thompson, J. D., Gibson, T. J. & Higgins, D. G. (2002). *Curr. Protoc. Bioinformatics*, ch. 2, Unit 2.3.
Tsai, C.-H. & Ho, C. (2002). *Biophys. Chem.* **98**, 15–25.
Weber, R. E., Jessen, T. H., Malte, H. & Tame, J. (1993). *J. Appl. Physiol.* **75**, 2646–2655.
Zhang, J., Hua, Z., Tame, J. R., Lu, G., Zhang, R. & Gu, X. (1996). *J. Mol. Biol.* **255**, 484–493.